Video Article

Self-assembling Morphologies Obtained from Helical Polycarbodiimide Copolymers and Their Triazole Derivatives

Oleg V. Kulikov[1], Dumindika A. Siriwardane[1], Gregory T. McCandless[1], Samsuddin F. Mahmood[1], Bruce M. Novak[1]

[1]Department of Chemistry and Biochemistry, University of Texas at Dallas

Correspondence to: Oleg V. Kulikov at oleg.kulikov.chem@gmail.com, Bruce M. Novak at bxn111230@utdallas.edu

URL: https://www.jove.com/video/55124
DOI: doi:10.3791/55124

Keywords: Chemistry, Issue 120, helical polycarbodiimides, self-assembly in thin film, atomic force microscopy, scanning electron microscopy, *graft*-polystyrene, secondary structure, "click" reaction

Date Published: 2/7/2017

Citation: Kulikov, O.V., Siriwardane, D.A., McCandless, G.T., Mahmood, S.F., Novak, B.M. Self-assembling Morphologies Obtained from Helical Polycarbodiimide Copolymers and Their Triazole Derivatives. *J. Vis. Exp.* (120), e55124, doi:10.3791/55124 (2017).

Abstract

A facile method for the preparation of polycarbodiimide-based secondary structures (*e.g.*, nano-rings, "craters," fibers, looped fibers, fibrous networks, ribbons, worm-like aggregates, toroidal structures, and spherical particles) is described. These aggregates are morphologically influenced by extensive hydrophobic side chain-side chain interactions of the singular polycarbodiimide strands, as inferred by atomic force microscopy (AFM) and scanning electron microscopy (SEM) techniques. Polycarbodiimide-*g*-polystyrene copolymers (PS-PCDs) were prepared by a combination of synthetic methods, including coordination-insertion polymerization, copper(I)-catalyzed azide alkyne cycloaddition (CuAAC) "click" chemistry, and atom transfer radical polymerization (ATRP). PS-PCDs were found to form specific toroidal architectures at low concentrations in $CHCl_3$. To determine the influence of a more polar solvent medium (*i.e.,* THF and THF/EtOH) on polymer aggregation behavior, a number of representative PS-PCD composites have been tested to show discrete concentration-dependent spherical particles. These fundamental studies are of practical interest to the development of experimental procedures for desirable architectures by directed self-assembly in thin film. These architectures may be exploited as drug carriers, whereas other morphological findings represent certain interest in the area of novel functional materials.

Video Link

The video component of this article can be found at https://www.jove.com/video/55124/

Introduction

The helix is a ubiquitous chiral motif observed in nature. Complex biological systems and their components, such as proteins, polypeptides, and DNA, all utilize the helical structure as a means of performing complex tasks for applications like information storage, tissue molecular transportation support, and localized chemical transformations.

Helical polymeric macromolecules[1] have been a target for the design of functional materials and composites possessing interesting properties, which enabled their practical use in many areas[2,3,4,5]. So far, numerous helical scaffolds[6,7,8,9], as well as their secondary structure motifs, have been successfully exploited to achieve promising results, both in the field of physical engineering[10,11,12] and in biological applications[13,14]. Current studies represent a logical extension of our earlier efforts to synthesize optically active alkyne polycarbodiimides bearing one or two modifiable alkyne moieties per repeat unit[15,16,17].

Recently, we reported[22] the homo- and co-polymerization of carbodiimide monomers leading to chiral helical macromolecules — a family of (*R*)- and (*S*)-polycarbodiimides with modifiable pendant groups that offer further functionalization through a CuAAC "click" protocol. Br-terminated polycarbodiimides obtained from their respective ethynyl precursors were shown to act as ATRP macroinitiators in *graft*-polymerization with styrene[23].

The specific aim of this manuscript is to provide a practical guide for morphological characterizations (AFM measurements and SEM inspection) of the secondary structures formed from PS-PCDs synthesized from their corresponding ethynyl precursors by using a well-known click protocol[21]. In particular, experimental details, such as the solvent of choice, the temperature, the deposition method, the substrate chosen for deposition, and the polymer structure, were shown to be highly important to obtain specific morphologies (*e.g.*, fibers, including right- and left-handed helical senses; nano-spheres; and nano-rings). They may also be of use for the development of materials with tunable properties based on polycarbodiimides with precisely controlled chiral architecture.

Protocol

NOTE: All reactions were performed in a glove box (or fume hood, when noted) using standard scintillation vials.

1. Synthesis of the (*R*)- and (*S*)-series of Ethynylpolycarbodiimides

1. Place 1.0 g (0.00442 mol) of *N*-(3-ethynylphenyl)-*N'*-hexylcarbodiimide monomer (**ET**) and 0.894 g (0.00442 mol) of *N*-phenyl-*N'*-hexylcarbodiimide monomer (**Ph**) as transparent, viscous liquids in a clean scintillation vial (20 mL) with a magnetic stirring bar (glove box) to obtain a representative ***R*-50-ET-50-Ph** composition.
   NOTE: Use only one monomer to generate the respective homopolymers. Mixing two monomer precursors at different ratios afforded a library of random copolymers[22].
2. Weigh out 0.018 g (0.00004 mol) of (*R*)- BINOL Ti(IV) diisopropoxide catalyst as a red (sometimes orange), fine powder material in a glove box (monomer-to-catalyst molar ratio is 250:1) and add it to the scintillation vial.
3. Add ~3-5 mL of anhydrous $CHCl_3$ to dissolve both the monomer and the catalyst. Gentle stirring may be required at this step to dissolve the catalyst, which may otherwise form chunks of material. Perform all manipulations with reagents under an inert atmosphere (glove box) at 25 °C.
4. Cap the scintillation vial containing all the reagents and allow the reaction mixture to stir overnight at 25 °C in a glove box.
5. Remove the magnetic bar and add ~5 mL of additional $CHCl_3$ to re-dissolve the dark red, viscous material (outside the glove box).
6. Inject the solution obtained in the previous step into cold MeOH (250 mL) containing 0.5 mL of 1,8-diazabicyclo[2.5.0]undec-7-ene (DBU) to precipitate the polymer material as yellowish fibers.
7. Collect the polymer formed by filtration (fritted funnel, 15 mL, 4-8 µm) and wash it with MeOH (~10 mL, 3x).
8. Re-dissolve the material obtained from the previous step in $CHCl_3$ and re-precipitate it in MeOH to remove the residual Ti(IV)-BINOL catalyst. Dry the precipitate under high vacuum (200 mTorr) for 24 h to remove the MeOH. Repeat this procedure once to ensure the purity of the resulting polymer.

2. Synthesis of the (*R*)- and (*S*)-series of Triazole Polycarbodiimides under a "Click" Protocol

1. Add 5 mL of anhydrous THF (glove box) and a magnetic stirring bar to the scintillation vial (20 mL) containing 0.25 g (0.00117 mol) of ***R*-50-ET-50Ph** to synthesize a representative ***R*-50-TRZ-50-Ph** composition.
2. Weigh out 0.146 g (0.00059 mol) of *N*-(3-azidopropyl)-2-bromo-2-methylpropane amide[22] in the glove box and add it to the scintillation vial.
3. Weigh out 0.022 g (0.00012 mol) of Cu(I) iodide catalyst in the glove box and load it into the scintillation vial. Let the solution stir for 2 min to form a homogeneous suspension.
4. Charge the same vial with 0.713 g (0.00468 mol) of DBU, cap the vial, and allow it to stir for 2 h in the glove box at 25 °C (avoid a longer reaction time to prevent hard gel formation).
5. Remove the magnetic bar and inject the reaction mixture (greenish gel-like solution) obtained in step 2.4 into cold MeOH (250 mL) containing 0.5 mL of DBU (outside the glove box).
6. Collect the formed triazole polymer by filtration (fritted funnel, 15 mL, 10 µm) and wash it with MeOH.
7. Repeat purification step 2.6 (*i.e.*, dissolution in THF and precipitation from MeOH) one more time to remove the residual catalyst.
8. Dry the product of the "click" reaction under a high vacuum (200 mTorr) for 24 h to remove traces of MeOH.

3. Synthesis of the (*R*)- and (*S*)-series of Polycarbodiimide-*g*-polystyrene Copolymers

1. Mix 0.029 g (0.00029 mol) of Cu(I) chloride catalyst with 0.1 g (0.00029 mol) of ***R*-50-TRZ-50Ph** macroinitiator in the scintillation vial (20 mL) containing 0.101 g (0.00058 mol) of *N*,*N*,*N'*,*N'*,*N''*-pentamethylenediethylenetriamine (PMDETA). Place a magnetic stirring bar into the vial (glove box) to obtain a representative ***R*-50-TRZ-50Ph-*graft*-polystyrene** copolymer.
2. Charge a vial from step 3.1 with 1.510 g (0.0145 mol) of freshly distilled styrene.
3. Add ~12 mL of anhydrous toluene (or DMF)[23] into the vial from step 3.2 to dissolve the reagents; seal the vial tightly before taking it out of the glove box.
4. Within a fume hood, immerse the sealed vial in an oil bath and increase the temperature. Once the temperature reaches the desired value (temperature may vary from 57 to 100 °C, depending on the particular copolymer)[23], maintain it for 12 h (actual reaction time may range from 6 h to 4 days, depending on the experiment).
5. Remove the vial from the hot plate and cool the white, viscous material down to 25 °C.
6. Take the reaction vessel with resulting solid out of the glove box.
7. Unscrew the vial, remove the stirring bar, and pour the reaction mixture into 250 mL of cold MeOH containing 0.5 mL of DBU.
8. Collect the formed flakes of PS-PCDs by filtration (fritted funnel, 15 mL, 4-8 µm) and wash the material with cold MeOH (discard the supernatant left after filtration).
9. Repeat purification step 3.8 (*i.e.*, dissolution in DMF and precipitation from MeOH) one more time to remove the residual catalyst.
10. Dry the material (white powder) under a high vacuum (200 mTorr) for 24 h to remove the MeOH.

4. Thin-film Preparation for Tapping Mode Atomic Force Microscopy (TMAFM) Measurements

1. Weigh 10 mg of polymeric material and place it in a 5-mL vial.
2. Add 1 mL of the solvent of choice (*e.g.*, $CHCl_3$ or THF) into the vial and vortex the polymer suspension to dissolve the material.
   NOTE: Some polymer compositions require an extended period of standing time (~6 h) to completely dissolve the polymer.
3. Perform a successive dilution (*i.e.*, using more dilute solutions at each step as the "stock") to prepare a series of stocks of 5.0, 2.5, 1.25, 0.625, 0.313, and 0.156 mg/mL concentrations.
4. Filter the stock solution through a 0.45-µm PTFE syringe filter prior to deposition on the silicon wafer (200 µL) with the following specifications (diam.: 25.4 ± 0.5 mm; orientation: 100 ± 0.5°; thickness: 250-300 µm; surface: single-side polished; type: N/Phos).

NOTE: The deposited solution must cover the entire area of a silicon wafer.

5. Use a spin-coating machine immediately after depositing the sample (1 min, 1,000 rpm) to cover the entire wafer surface with a uniform polymeric film).
6. Acquire AFM images at 25 °C by using silicon cantilevers with nominal spring constants of 42 N/m, nominal resonance frequencies of 320 kHz, and standard silicon OTESPA or OTESPA-R3 tips (*e.g.*, OTESPA-R3 material: 0.01-0.02 ohm-cm silicon, cantilever: T: 3.7 µm, f_o: 300 kHz, L: 160 µm, k: 26 N/m, W: 40 µm). Vary the amplitude set-point values from 425 to 273 mV, with scan rates of 0.99 and 1.99 Hz, respectively[22,23].
   NOTE: The experimental details for SEM specimen preparation and image acquisition were discussed earlier[23].

Representative Results

Figure 1 (upper panel) illustrates BINOL (*R*)- or (*S*)-titanium (IV) catalyst-mediated coordination-insertion polymerization leading to the (*R*)- and (*S*)-series of ethynylpolycarbodiimides with an altering ratio of the repeat units (*i.e.*, aryl- and alkyne aryl). Monomers and catalysts were obtained as described elsewhere[18]. Both (*R*)- and (*S*)-family alkyne random copolymers were selected for "click"-coupling with *N*-(3-azidopropyl)-2-bromo-2-methylpropane amide[22]. The lower panel shows the synthesis of the triazole polycarbodiimides used as macroinitiators in the ATRP reaction to produce polycarbodiimide-*g*-polystyrenes (PS-PCDs)[22,23].

Figure 2 illustrates a model of the polycarbodiimide backbone, depicted as a pink spiral spinning around the yellow axis. Brown and green substituents form a "secondary" helical motif with respect to the pink amidine main chain. Macromolecules can self-assemble in a thin film to form a great variety of complex supramolecular architectures, such as fibers, looped fibers, superhelices, fibrous networks, ribbons, worm-like aggregates, toroidal structures, and craters. A molecular model of the triazole macroinitiator is given in **Figure 3** (35-mer segment of a polymer chain with terminal Br atoms represented in red).

Figures 4 and **5** show the representative AFM images of alkyne PCDs, confirming the formation of fiber-like morphologies and their respective diameter sizes (*e.g.,* **Figure 5**: ~76 nm (panel b), 38-60 nm (panel c), 30-40 nm (panel e), and ~12-20 nm (panel f)). In general, diluting stock solutions resulted in diminishing the size of the aggregated morphologies formed (*e.g.*, "thick," fiber-like networks at relatively high concentrations tend to transform into thin, separated fibers upon dilution).

Also shown are the morphologies formed from polycarbodiimide-*g*-polystyrenes spin-coated from $CHCl_3$ stock (**Figure 6**). Unlike alkyne polycarbodiimide aggregation behaviors in $CHCl_3$, examining PS-PCDs revealed both crater-like assemblies and nano-size toroidal architectures as predominant motifs. The reproducible formation of those morphologies is thought to be driven by concentration changes.

Figures 7 and **8** both illustrate representative AFM images of polycarbodiimide-*g*-polystyrenes indicative of the formation of discrete nano-spheres when applying a THF or binary THF/EtOH (25%, v) solvent system for sample deposition with concentration-dependent particle sizes. **Figure 8** shows the assembly of the individual macromolecules into spherical nano-particles of ~84 nm in size matching up closely SEM-measured morphologies (~100 nm, panel e). Remarkably, the greater micron-size aggregates shown in panels a-d may be comprised of individual nano-particles agglomerated together.

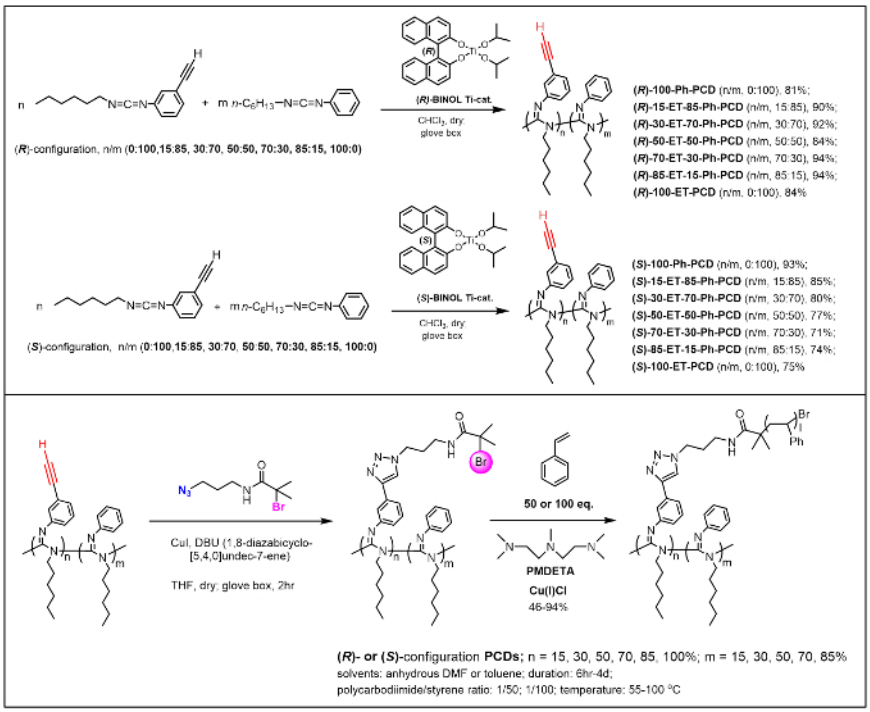

Figure 1. Synthesis of alkyne polycarbodiimides and their "grafting from" transformation to PS-PCDs. (*R*)- and (*S*)-series of ethynylpolycarbodiimides were generated by altering the ratio of carbodiimide precursors (*i.e.*, *N*-phenyl-*N'*-hexylcarbodiimide monomer (**Ph**) and *N*-(3-ethynylphenyl)-*N'*-hexylcarbodiimide (**ET**)), with repeat unit compositions varying in the range: 0:100 (**100-Ph**), 15:85 (**15-ET-85-Ph**), 30:70 (**30-ET-70-Ph**), 50:50 (**50-ET-50-Ph**), 70:30 (**70-ET-30-Ph**), 85:15 (**85-ET-15-Ph**), and 100:0 (**100-ET**). The "click" protocol was used to synthesize their triazole derivatives, which were further employed as Br-terminated macroinitiators for the ATRP reaction with styrene (either 50 or 100 eq.) to form polycarbodiimide-*g*-polystyrenes. Reprinted with permission[22]. Please click here to view a larger version of this figure.

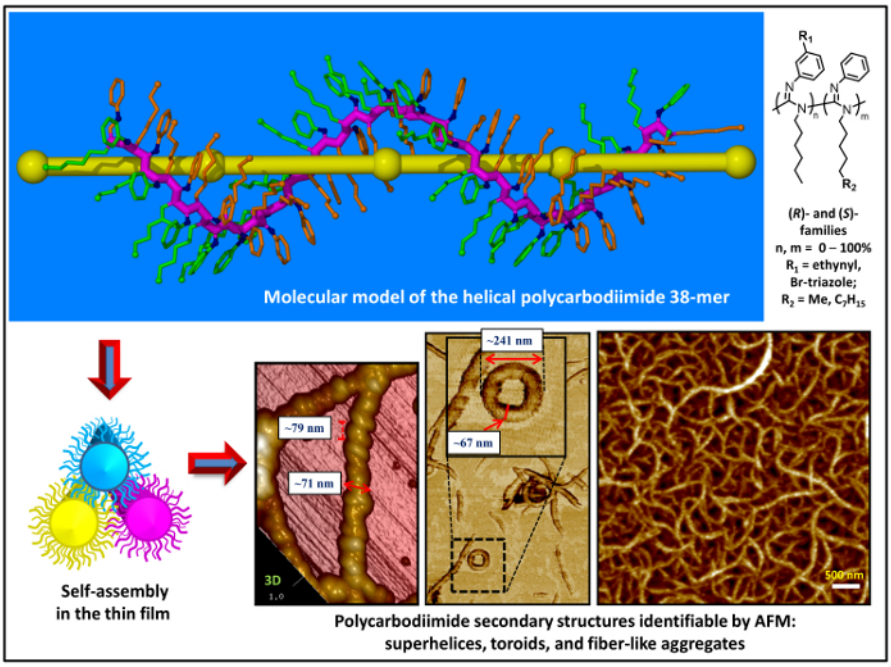

Figure 2. Schematic representation of polycarbodiimides self-assembling into fibrillar motifs. The panels show the representative helical macromolecule and self-assembly of individual macromolecules to form bundled structures identifiable by AFM analysis. Reprinted with permission[22]. Please click here to view a larger version of this figure.

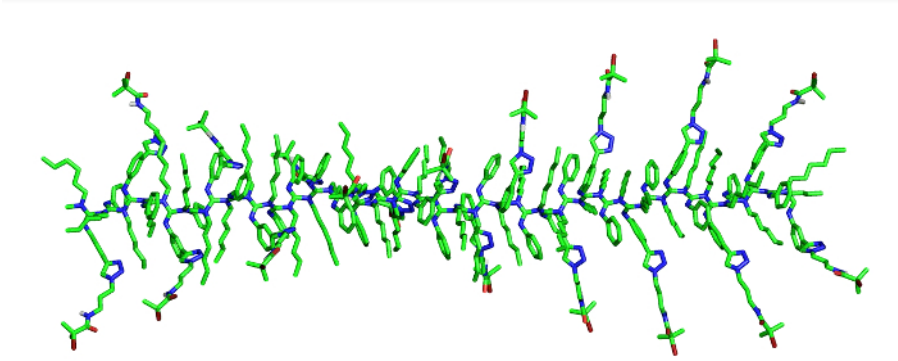

Figure 3. Molecular model of triazole polycarbodiimide. The triazole polycarbodiimide structure displays the helical motif introduced by specific orientations of Br-terminated side chains. Atom color codes: carbon (green), nitrogen (blue), oxygen (red), and bromine (red). Please click here to view this video. (Right-click to download.)

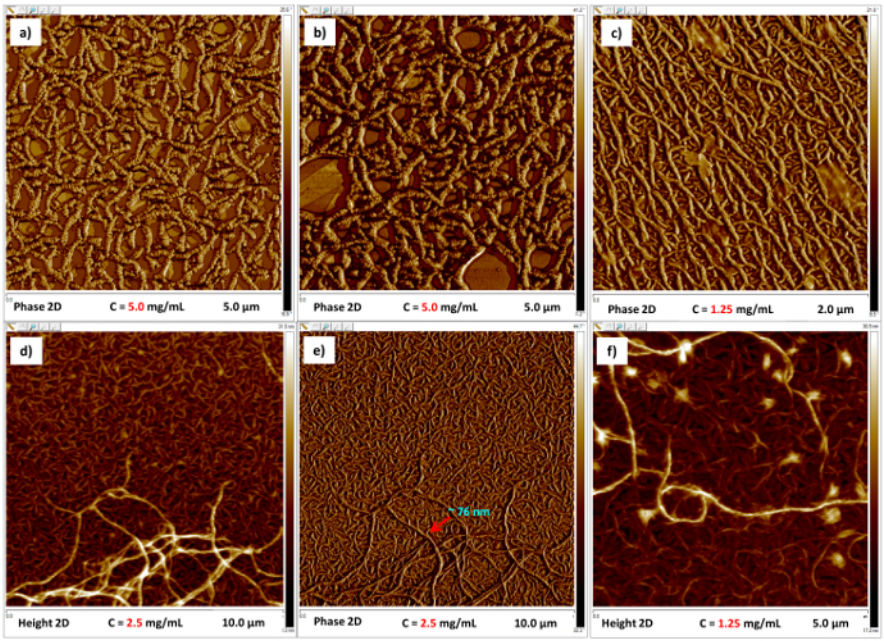

Figure 4. Evidence for alkyne polycarbodiimide fiber formation by AFM. Fibrous aggregates appeared to be a common trend for all alkyne composites. Representative AFM micrographs are taken for (*S*)-85-ET-15-Ph-PCD (**panels a-c**) and (*S*)-100-ET-PCD (**panels d−f**) polymers deposited from $CHCl_3$. Reprinted with permission[22]. Please click here to view a larger version of this figure.

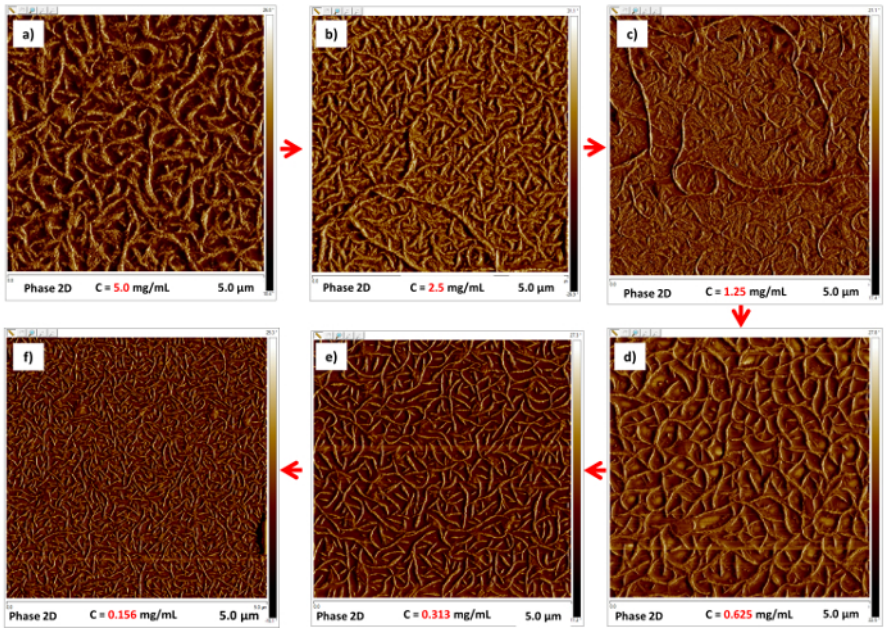

Figure 5. Controlling the size/thickness of fibers through concentration change. Fibrous aggregates are generated from (*S*)-100-ET-PCD at different concentrations: 5.0 mg/mL (**panel a**); 2.5 mg/mL (**panel b**); 1.25 mg/mL (**panel c**); 0.625 mg/mL (**panel d**); 0.313 mg/mL (**panel e**); and 0.156 mg/mL (**panel f**), deposited from $CHCl_3$. Scan size = 5.0 x 5.0 µm. Please click here to view a larger version of this figure.

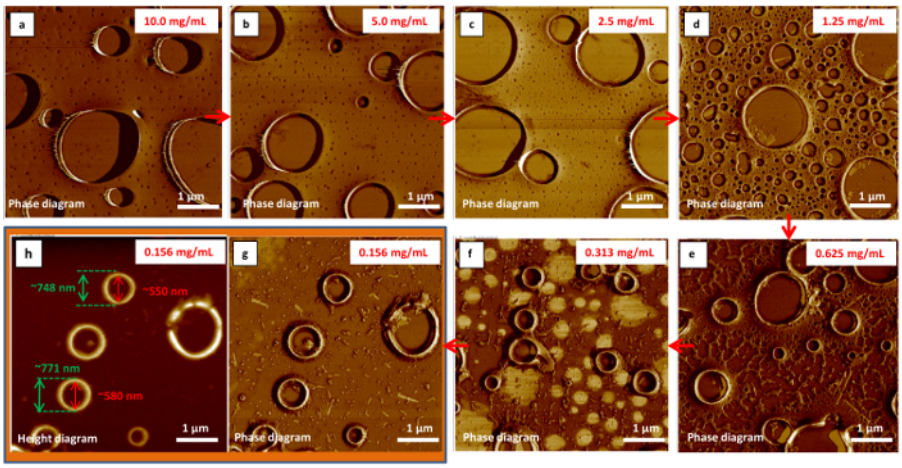

Figure 6. Developing PS-PCD nano-ring patterns in the thin film. Representative concentration series for (*R*)-30-TRZ-70-Ph-STYR(1:100)-PCD polymer: 10.0 mg/mL (**panel a**); 5.0 mg/mL (**panel b**); 2.5 mg/mL (**panel c**); 1.25 mg/mL (**panel d**); 0.625 mg/mL (**panel e**); 0.313 mg/mL (**panel f**); and 0.156 mg/mL (**panels g and h**). Scan size = 5.0 x 5.0 µm. Reprinted with permission[23]. Please click here to view a larger version of this figure.

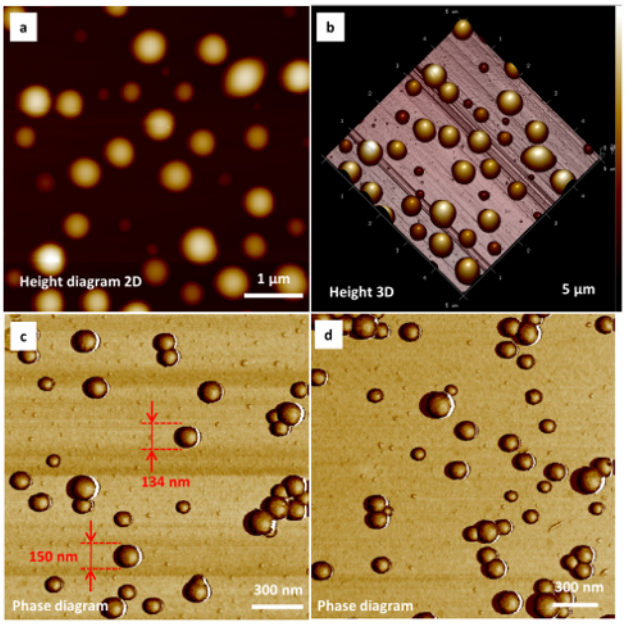

Figure 7. Polycarbodiimide-*g*-polystyrene nano-particles assembled in the thin film. Representative height and phase diagrams for (*S*)-50-TRZ-50-Ph-STYR(1:50)-PCD polymer in different solvents: THF (**panels a, b**) and THF/EtOH binary system (**panels c, d**). Importantly, appending PS-segments to the polycarbodiimide backbone has a noticeable effect on the self-assembling properties; thus, macromolecules tend to aggregate into "craters" and nano-rings rather than fibers, a predominant motif found for all alkyne PCDs. Reprinted with permission[23]. Please click here to view a larger version of this figure.

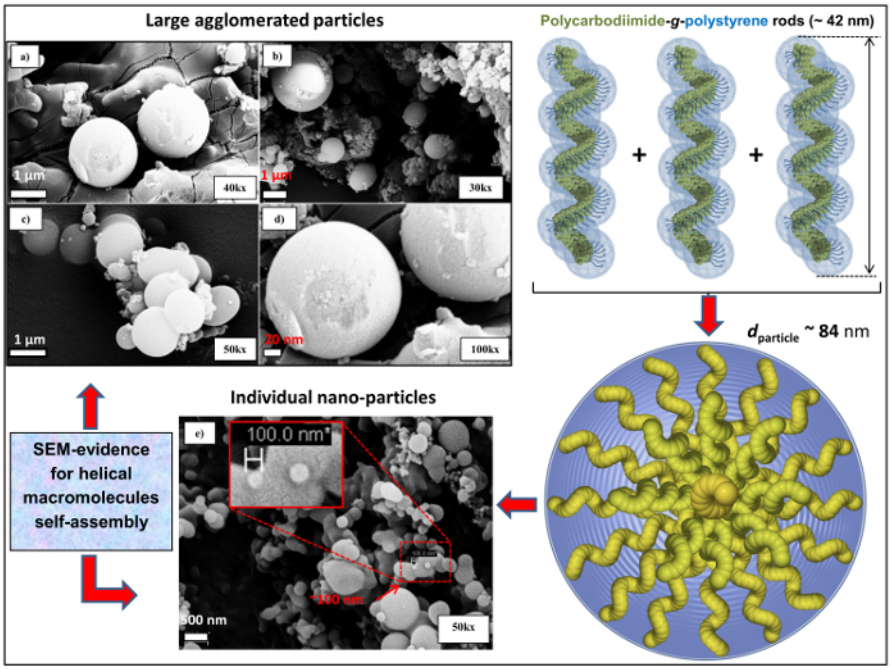

Figure 8. Schematic representation of polycarbodiimide-*g*-polystyrene nano-spheres as evidenced by SEM-analysis. Individual nano-particles (**panel e**) and large aggregates (**panels a-d**) assembled from (*S*)-70-TRZ-30-Ph-STYR(1:100)-PCD and (*R*)-50-TRZ-50-Ph-STYR(1:100)-PCD polymers, respectively. Proposed self-assembly model for the individual polycarbodiimide-*g*-polystyrene macromolecules with rigid polycarbodiimide backbones (green-yellow) dispersed in the environment and formed by polystyrene lateral chains (light blue). Reprinted with permission[23]. Please click here to view a larger version of this figure.

Discussion

In summary, the spin-coating deposition method represents a convenient way to reproducibly generate multiple-type morphologies, including fiber-like aggregates, ribbons, worm-like structures, fibrillar networks, looped fibers, toroids, and superhelices, from either alkyne polycarbodiimides or from their respective PS-derivatives (*i.e.*, polycarbodiimide-*g*-polystyrenes). Thus, coordination-insertion polymerization,

along with further functionalization using a "click" reaction followed by ATRP, provides a unique opportunity to rapidly obtain a series of statistical polycarbodiimides with the *R*- and *S*-configuration of backbones in a nearly quantitative yield.

Alkyne polycarbodiimide formation (**Figure 1**) appears to be a critical step in polymer synthesis, since those macromolecules are important as substrates for the production of fiber-like aggregates; they also serve as precursors in the synthesis of polycarbodiimide-*g*-polystyrenes. Notably, alkyne compositions with a high n:m ratio tend to produce completely insoluble (or having very limited solubility in organic solvents) material during the course of Cu(I)-catalyzed "click" synthesis, possibly as a result of the cross-linking side reaction. Unlike the most common C_6-residues, longer dodecyl alkyl chains (*i.e.*, C_{12}-) having increased conformational flexibility should be avoided from a practical point of view, since they often lead to the formation of complex dewetting patterns and "craters" rather than distinct individual fibers[22].

Another important practical finding for both alkyne PCD and PS-PCD series is their ability to form secondary structures that are strongly influenced by solvent and concentration (*i.e.*, control over the type and dimensions (or size) of aggregated morphologies), thus opening up possibilities for the structural design and preparation of novel functional materials based on rigid-rod polycarbodiimides. Specifically, toroidal aggregates can be successfully obtained from polycarbodiimide-*g*-polystyrenes when spin-coated from 0.156 mg/mL $CHCl_3$ stock (**Figure 6**), whereas applying the more polar THF or THF/EtOH (25% by volume) solvent system to the grafted macromolecules induces the formation of spherical aggregates, as shown by the combination of AFM and SEM techniques (**Figures 7** and **8**). Despite the fact that there is no linear relationship between the concentration and diameter of the fibers/ribbons formed when spin-coated from $CHCl_3$ on an Si wafer, it seemed that decreasing the concentration of stock solution allowed for control of the thickness of the fibrous morphologies for alkyne PCDs (**Figure 5**).

Limitations in the provided method arise from the technique itself used to generate nano-structures (*i.e.*, motifs easily identifiable by AFM in thin film by tapping mode may or may not retain their structure in solution or in bulk; however, in certain cases, it is possible to corroborate AFM findings with SEM measurements). Another disadvantage of using the AFM technique is the low uniformity of thin-film patterns. Therefore, the end result is often predetermined by a delicate balance of the polymer structure, solvent of choice, deposition method, and substrate. The latter requires thorough and careful screening of multiple specimens in order to define the optimal conditions for each specific morphological motif.

A key advantage of the aforementioned AFM technique is that it offers a reliable and inexpensive way to produce and visualize specific morphologies (*i.e.*, fibers, nano-rings, and spheres) assembled from statistical polycarbodiimide polymers with rigid backbones that are otherwise obtainable by more sophisticated methods, including the blending of chemically distinct polymers[24], applying surfactants, or using relatively complex machinery like microcapillary devices[25]. Future applications of this method might include developing the electronic nose[26], constructing spherical aggregates as carriers to deliver drug molecules[27], and designing novel liquid crystalline materials[28].

Disclosures

The authors have nothing to disclose.

Acknowledgements

We gratefully acknowledge the NSF-MRI grant (CHE-1126177) used to purchase the Bruker Advance III 500 NMR instrument.

References

1. Yashima, E., Maeda, K., Iida, H., Furusho, Y., Nagai, K. Helical Polymers: Synthesis, Structures, and Functions. *Chem. Rev.* **109**, 6102-6211 (2009).
2. Miyabe, T., Hase, Y., Iida, H., Maeda K., Yashima, E. Synthesis of functional poly(phenyl isocyanide)s with macromolecular helicity memory and their use as asymmetric organocatalysts. *Chirality*. **21**, 44-50 (2009).
3. Iida, H., Iwahana, S., Mizoguchi T., Yashima, E. Main-Chain Optically Active Riboflavin Polymer for Asymmetric Catalysis and Its Vapochromic Behavior. *J. Am. Chem. Soc.* **134**, 15103-15113 (2012).
4. Shimomura, K., Ikai, T., Kanoh, S., Yashima E., Maeda, K. Switchable enantioseparation based on macromolecular memory of a helical polyacetylene in the solid state. *Nat.Chem.*, **6**, 429-434 (2014).
5. Qi, S., et al. Electrical Switching Behavior of a [60]Fullerene-Based Molecular Wire Encapsulated in a Syndiotactic Poly(methyl methacrylate) Helical Cavity. *Angew. Chem. Int. Ed.*, **52**, 1049-1053 (2013).
6. Maeda, K., Wakasone, S., Shimomura, K., Ikai, T., Kanoh, S. Chiral Amplification in Polymer Brushes Consisting of Dynamic Helical Polymer Chains through the Long-Range Communication of Stereochemical Information. *Macromolecules*. **47**, 6540-6546 (2014).
7. Kikuchi, M., et al. Conformational Properties of Cylindrical Rod Brushes Consisting of a Polystyrene Main Chain and Poly(*n*-hexyl isocyanate) Side Chains. *Macromolecules*. **41**, 6564-6572 (2008).
8. Banno, M., et al. Optically Active, Amphiphilic Poly(*meta*-phenylene ethynylene)s: Synthesis, Hydrogen-Bonding Enforced Helix Stability, and Direct AFM Observation of Their Helical Structures. *J. Am. Chem. Soc.*, **134**, 8718-8728 (2012).
9. Jiang, Z., et al. One-Pot Synthesis of Brush Copolymers Bearing Stereoregular Helical Polyisocyanides as Side Chains through Tandem Catalysis. *Macromolecules*. **48**, 81-89 (2015).
10. Zhu, Y., et al. Synthesis and Chiroptical Properties of Helical Polyallenes Bearing Chiral Amide Pendants. *Macromolecules*. **47**, 7021-7029 (2014).
11. Kennemur, J. G., Novak, B. M. Advances in polycarbodiimide chemistry. *Polymer*. **52**, 1693-1710 (2011).
12. Arnold, L., Marx, A., Thiele, C. M., Reggelin, M. Polyguanidines as Chiral Orienting Media for Organic Compounds. *Chem. Eur. J.*, **16**, 10342-10346 (2010).
13. Kennemur, J. G., Clark, IV, J. B., Tian, G., Novak, B. M. A New, More Versatile, Optical Switching Helical Polycarbodiimide Capable of Thermally Tuning Polarizations ±359°. *Macromolecules*. **43**, 1867-1873 (2010).
14. Kim, J., Novak, B. M., Waddon, A. J. Liquid Crystalline Properties of Polyguanidines. *Macromolecules*. **37**, 8286-8292 (2004).

15. Budhathoki-Uprety, J., Peng, L., Melander, C., Novak, B. M. Synthesis of Guanidinium Functionalized Polycarbodiimides and Their Antibacterial Activities. *ACS Macro Lett.*, **1**, 370-374 (2012).
16. Heller, D. A., Budhathoki-Uprety, J. Helical Polycarbodiimide Cloaking of Carbon Nanotubes Enables Inter-Nanotube Exciton Energy Transfer Modulation. From *PCT Int. Appl. WO 2016028636 A1 20160225.* (2016).
17. Budhathoki-Uprety, J., Jena, P. V., Roxbury, D., Heller, D. A. Helical Polycarbodiimide Cloaking of Carbon Nanotubes Enables Inter-Nanotube Exciton Energy Transfer Modulation. *J. Am. Chem. Soc.* **136**, 15545-15550 (2014).
18. Budhathoki-Uprety, J., Reuther, J. F., Novak, B. M. Determining the Regioregularity in Alkyne Polycarbodiimides and Their Orthogonal Modification of Side Chains To Yield Perfectly Alternating Functional Polymers. *Macromolecules*. **45**, 8155-8165 (2012).
19. Budhathoki-Uprety, J., Novak, B. M. Synthesis of Alkyne-Functionalized Helical Polycarbodiimides and their Ligation to Small Molecules using Click and Sonogashira Reactions. *Macromolecules*. **44**, 5947-5954 (2011).
20. Wu, Z.-Q., et al. One pot synthesis of a poly(3-hexylthiophene)-*b*-poly(quinoxaline-2,3-diyl) rod-rod diblock copolymer and its tunable light emission properties. *Polym. Chem.* **4**, 4588-4595 (2013).
21. Barkey, N. M., et al. Development of Melanoma-Targeted Polymer Micelles by Conjugation of a Melanocortin 1 Receptor (MC1R) Specific Ligand. *J. Med. Chem.*, **54**, 8078-8084 (2011).
22. Kulikov, O. V., et al. Characterization of Fibrous Aggregated Morphologies and Other Complex Architectures Self-Assembled from Helical Alkyne and Triazole Polycarbodiimides (*R*)- and (*S*)-Families in the Bulk and Thin Film. *Macromolecules*. **48**, 4088-4103 (2015).
23. Kulikov, O. V., Siriwardane, D. A., McCandless, G. T., Mahmood, S. F., Novak, B. M. Self-assembly studies on triazolepolycarbodiimide-*g*-polystyrene copolymers. *Polymer*. **92**, 94-101 (2016).
24. Min, N. G., et al. Anisotropic Microparticles Created by Phase Separation of Polymer Blends Confined in Monodisperse Emulsion Drops. *Langmuir*. **31***,* 937-943 (2015).
25. Wang, B.; Shum, H. C.; Weitz, D. A. Fabrication of Monodisperse Toroidal Particles by Polymer Solidification in Microfluidics. *ChemPhysChem*. **10**, 641-645 (2009).
26. Gruber, J., et.al. A conductive polymer based electronic nose for early detection of Penicillium digitatum in post-harvest oranges. *Mater. Sci. Eng., C*. **33**, 2766-2769 (2013).
27. Percec, V., et al. Self-Assembly of Janus Dendrimers into Uniform Dendrimersomes and Other Complex Architectures. *Science*. **328**, 1009-1014 (2010).
28. Pathiranage, T. M. S. K., et al. Synthesis and characterization of side-chain thermotropic liquid crystalline copolymers containing regioregular poly(3-hexylthiophene). *Polymer*. **72**, 317-326 (2015).

